Progress of Theoretical Physics, Vol. 57, No. 3, March 1977

The Structure of ^{9}Be Nucleus by a Molecular Model. I†

Shigetō OKABE, Yasuhisa ABE* and Hajime TANAKA

Department of Physics, Hokkaido University, Sapporo 060
**Research Institute for Fundamental Physics, Kyoto University, Kyoto 606*

(Received October 15, 1976)

The nucleus ^{9}Be is investigated by an extended molecular-orbital model and by the generator coordinate method in the simple LCAO approximation. The Hartree-Fock calculations show that α-cluster structures are stable in intrinsic states and the degree of clustering depends crucially on motions of the valence neutron. The generator coordinate calculations give good descriptions of the energy level structures of normal and non-normal parity states in terms of rotational bands. Energy spectra of ^{9}B are given as well. A $K^\pi=1/2^-$ band is also predicted. The ground state properties, that is, r.m.s.-radius, Q-moment and μ-moment are reproduced as quite well as electric transitions and charge form factors for the members of the ground rotational band. It is concluded that the molecular model admirably succeeds in systematic explanation of the low energy properties of ^{9}Be. Comparisons are made with the simple shell model and the projected Hartree-Fock calculation by Bouten et al.

§ 1. Introduction

In the last 15 years, investigations of the cluster structures in light nuclei have been developed steadily from molecular viewpoints. It is found that a number of states in the light $4N$-selfconjugate nuclei, which include both normal and anomalous states in the shell model versions up to rather high excitation energies, can be successfully explained as some modes of cluster motions.[2a)]

Compared with $4N$-nuclei, odd-A and odd-odd nuclei have not been studied so well.[2b)] Especially as for $4N+1$-nuclei, a problem of the coupling of a valence nucleon to the motions of clusters has never been fully discussed in any nuclei. In this and forthcoming papers, ^{9}Be nucleus is taken up as a typical example in order to study the probelm, because the α-cluster structure of ^{8}Be is well established. The experimental data on this nucleus have been accumulated,[3)] not only about nuclear levels but also form factors for electron scattering which are able to give a definite test of model wave functions.

As shown in the middle column of Fig. 4, this nucleus has a clear ground rotational band and the moment of inertia is very close to that of ^{8}Be nucleus ($\hbar^2/2\mathcal{J}\simeq 0.49$ MeV), which denotes a certain large deformation. Slight et al.[4)] used an extended Nilsson model, which includes major shell mixings up to $N+6$, to analyze electromagnetic properties. They obtained a good fit to the ground

† The preliminary results were reported at the International Conference on Nuclear Physics,[1)] Munich Germany, 1973.

state charge form factor at low momentum transfers with a quite large deformation ($\eta = +5.3$). It was pointed out, however, that higher-order terms other than r^2Y_{20} must be added to the Nilsson potential to describe the properties of the $5/2^-$ state at 2.43 MeV and that the sort of deformation was a dumbbell of two α-particles. A projected Hartree-Fock (P.H.F.) calculation with large admixtures of higher major shells was made by Bouten et al.[5] They succeeded in reproducing the inelastic form factor to the 2.43 MeV level as well as the elastic charge and magnetic form factors. The charge distribution of their ground wave function has been found to be of a dumbbell type and to be almost the same as that obtained by the present investigation in § 5.

The above investigations from the shell model picture resulted in a simple conclusion that the ground rotational band in ^{9}Be was well described by a strong coupling of the valence neutron with the rotor of the two α-particles. On the basis of the ground state structure, we can expect a variety of excited states as results of various couplings of the valence neutron with α-cluster motions, even though some of them may be unstable against particle decays. The non-normal parity levels observed in ^{9}Be can be considered to be such states. They, especially the $1/2^+$ state, appear at extremely low excitation energies, which are very difficult to understand within the shell model picture. A weak-coupling model, where the valence neutron is coupled to the motion of ^{8}Be core, was applied by several authors[6] to the non-normal parity levels, apart from the normal ones. They were successful in reproducing the energy spectra, but failed in explaining electron scattering data.

From the molecular viewpoints, Kunz[7] first carried out a calculation in a cluster model consisting of two α-particles plus a neutron with some success. He succeeded in reproduction of the normal parity levels, but failed in the quadrupole moment and the charge form factors. Hiura and Shimodaya[8] showed that too large a quadrupole moment was reduced by a dynamical treatment of the relative motion between the α-particles. Neudatchin et al.[9] extracted the degree of cluster separation by analyzing the charge form factors. As shown in a later section, the elastic charge form factor is improved by a microscopic treatment.

The purpose of the present paper is to investigate all the low energy properties of ^{9}Be systematically from the molecular viewpoints, that is, from the various couplings of the valence neutron with motions of the two α-clusters. For this purpose, a molecular-orbital model[10] is extended to odd-A nuclei, where the orbitals of the valence nucleon are approximated by the simple linear combination of "atomic" orbitals (LCAO) and the Pauli principle is exactly taken into account among all the nucleons. The molecular-orbital model is recapitulated in § 2. In § 3, the stability of α-cluster structures in ^{9}Be is investigated under the presence of the odd neutron. In § 4, adiabatic solutions are given at each cluster separation. Further, relative motions of α-clusters are solved under the presence of coupled neutron motions by the generator coordinate method (GCM), as zero-point oscil-

lations are important in molecule-like structures. The electromagnetic properties of the ground rotational band are discussed in § 5. Conclusions are given in § 6.

§ 2. Formulation

The molecular-orbital model is extended to odd-A systems, which has been devised in order to investigate the stability of α-cluster structure in $4N$-nuclei. In the model single-particle wave functions are expanded in terms of "atomic" orbitals around cluster centers, for which harmonic oscillator wave functions are taken for convenience' sake. They are classified according to the irreducible representations of the group corresponding to the imposed symmetry. The orthonormalized orbitals constructed with the two-center basis are given in the Appendix.

The total intrinsic wave functions, $\Phi_{K\pi\tau_z}$ or $\Phi_{K\tau_z}$, where K, π, and τ_z are the projection along the symmetry axis of the total angular momentum, the parity and the z-component of the isospin respectively, are constructed in Slater determinants, for example,

$$\Phi_{3/2^-,-1/2}=1/\sqrt{9!}\,\det|\phi_+^4(0s)\phi_-^4(0s)\phi_{3/2^-}(0p,0\ 1/2\ -1/2)|,$$
$$\Phi_{1/2^+,-1/2}=1/\sqrt{9!}\,\det|\phi_+^4(0s)\phi_-^4(0s)\phi_{1/2^+}(0p,0\ 1/2\ -1/2)|. \qquad (1)$$

In the simple LCAO approximation the wave function of ^{8}Be is the same as that of Brink's α-particle model[11] and an orbital of the valence neutron is represented by $\phi_{\Omega\pi}(0p)$ as in Eq. (1). The size parameter of atomic orbitals $b=\sqrt{\hbar/M\cdot\omega}$ and the cluster separation S are treated as variational parameters.

In order to investigate the stability of α-cluster structure the Hartree-Fock (H.F.) calculations are carried out in § 3. In odd-A system the so-called self-consistent symmetry[12] does not exist any more, but we define a single-particle Hamiltonian, $\bar{h}_{\text{s.p.}}(\phi)$, where the time reversal symmetry is conserved, and take it as an H.F. Hamiltonian.

$$\bar{h}_{\text{s.p.}}(\phi)=1/2(h(\phi)+h(\phi^T)). \qquad (2)$$

Here $h(\phi)$ and $h(\phi^T)$ are the H.F. Hamiltonian usually used, corresponding to Φ and $T\Phi$ respectively, where Φ is an intrinsic state and T is the time reversal operator and therefore $\bar{h}_{\text{s.p.}}(\phi)$ does not correspond to a single Slater determinant. The actual calculations are made in the truncated space up to p-shells around the cluster centers.

In § 4, relative motions are dealt with by the GCM, where the wave functions in the simple LCAO approximation are used as basis ones and the cluster separation S is taken as a generator coordinate. These wave functions include spurious states of the center-of-mass (c.m.) motion. Such components are removed by projection onto the ground state,

$$|\overline{\Phi_{K\pi\tau_z}(S)}\rangle=|(0s)\text{c.m.}\rangle\langle\langle(0s)\text{c.m.}|\Phi_{K\pi\tau_z}(S)\rangle, \qquad (3)$$

where $\rangle$ and $\langle$ represents integrations with respect to c.m. coordinates.

The total nuclear wave function with good angular momentum J and parity π is

$$|\Psi_M^{J\pi}\rangle = \Sigma_K \int_0^\infty dS f_K^{J\pi}(S)\, P_{MK}^J |\overline{\Phi_{K\pi\tau_z}(S)}\rangle\rangle , \qquad P_{MK}^J = \frac{2J+1}{8\pi^2}\int d\Omega D_{MK}^{J*}(\Omega)\, R_\Omega . \tag{4}$$

Eigenvalues and weight functions $f_K^{J\pi}(S)$ are determined by the Hill-Wheeler equation,[13]

$$\Sigma_{K'}\int dS' f_{K'}^{J\pi}(S')\langle J^\pi MK\tau_z(S)|H-E|J^\pi MK'\tau_z(S')\rangle = 0 , \tag{5}$$

where in practical calculations we take a finite linear combination of trial wave functions instead of the integral.

We used the following Hamiltonian:

$$H = T - T_{\text{c.m.}} + V_c + V_{so} . \tag{6}$$

T is the sum of single-particle kinetic energy operators and $T_{\text{c.m.}}$ is the kinetic energy of the c.m. motion and V_c consists of the Coulomb interaction and a central two-body force, for which Volkov No. 2[14] is used,

$$V(r_{ij}) = (1-m+mP_{ij}^r)\,(60.14e^{-(r_{ij}/1.01)^2} - 60.65e^{-(r_{ij}/1.80)^2}), \tag{7}$$

where P_{ij}^r is the Majorana exchange operator and the depths are in MeV and the ranges in fm. This force gives right binding energy for ^{4}He and ^{16}O at $m=0.60$. As for the spin-orbit interaction V_{so}, we use a one-body type or a two-body type,

$$V_{so} = -\xi\textstyle\sum_i \boldsymbol{l}_i\boldsymbol{s}_i \quad \text{or} \quad \sum_{i<j} V_{LS}((1-P_{ij}^r)/2)\,(e^{-(r_{ij}/0.4472)^2} - e^{-(r_{ij}/0.6)^2}), \tag{8}$$

where the depth V_{LS} is inferred to 900 MeV in nuclear matter by Nagata.[15] The values of the parameters m, V_{LS} and the optimum values of b are listed in Table I.

Table I. The parameter sets.

	m	V_{LS}(MeV)	b(fm)
Set I	0.60	800	1.46
Set II	0.57	620	1.39

In § 5, the charge form factors to the ground rotational band are discussed. They are defined as follows:[16]

$$|F(q^2)|^2_{i\to f} = \frac{1}{z^2(2I_i+1)}\Sigma_{M_iM_f}\left|\langle I_fM_f|\textstyle\sum_j \frac{1+\tau_z(j)}{2} e^{i\boldsymbol{q}\boldsymbol{r}_j}|I_iM_i\rangle\right|^2 . \tag{9}$$

The correction for the c.m. motion is done by multiplying $|F|$ with the factor, $e^{(q^2b^2/36)}$, for the c.m. motion remains in the ground state of a harmonic oscillator and the correction for the finite proton size is approximately made by multiplying $|F|$ with the factor $e^{(-q^2b_p^2/4)}$, where $\sqrt{3/2}b_p = 0.813$ fm is the proton r.m.s.-radius.

§ 3. Stability of α-cluster structure

Before discussing nuclear spectra, we investigate an average nuclear field with α-cluster structure in the H.F. approximation. To start with, diagonal energy curves are shown in Fig. 1, where total intrinsic wave functions are constructed in the simple LCAO approximation as in Eq. (1). It is readily seen that they have minima at cluster separations equal to about 2.7 fm and 3.7 fm for the normal and non-normal parity states respectively. This indicates that the degree of clustering changes correspondingly to the motions of the valence neutron, because the total parity is essentially determined by the single-particle orbital of the neutron. The total energy at each minimum point is also minimized with respect to the size parameter b. The value of b is equal to about 1.46 fm, which is larger than that of a free α-particle ($b=1.37$ fm, for the same force). Thus α-clusters in ^{9}Be polarize in a monopole type.

For the purpose of examining the stability of average nuclear fields with the above α-cluster structures, we carry out the H.F. calculations in the vicinity of the minimum points. The results are shown also in Fig. 1. The solutions obtained with the starting density of $\alpha+^5$He configurations are almost the same as those in the truncated space conserving the parity. This shows that a mixing of the parity in the single-particle orbitals is not necessary. The energy gains due to the H.F. calculations are quite small at the minimum points; $\Delta E^-\simeq 0.5$ MeV and $\Delta E^+\simeq 2.0$ MeV. The overlaps are very large between the H.F. solutions and the simple LCAO wave functions. It is noticed here that there is some difference between the normal and the non-normal parity states. As is seen in Fig. 1, the energy curve for the non-normal parity state remains steep at small cluster separa-

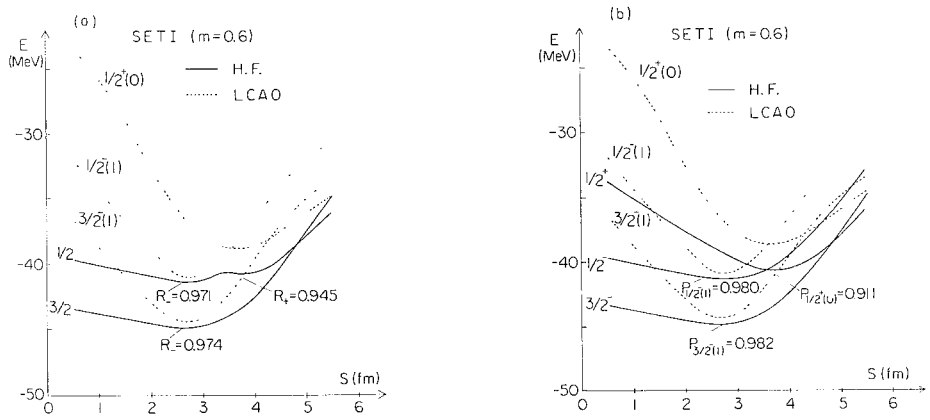

Fig. 1. Total intrinsic energy curves. (a) H.F. results carried out in the space mixing the parity. $1/2^+(0)$ denotes $K^\pi(A)$. $R_\pm=(1\pm\langle\Phi_{\text{H.F.}}|P|\Phi_{\text{H.F.}}\rangle)/2$, where P is a parity operator. (b) H.F. results carried out in the truncated space conserving the parity. $P_{K^\pi(A)}=|\langle\Phi_{K^\pi(A)}|\Phi_{\text{H.F.}}\rangle|^2$. $\Phi_{K^\pi(A)}$ is the wave function in the simple LCAO approximation. The values of $R_\pm$ and $P_{K^\pi(A)}$ given in the figure are those at minima.

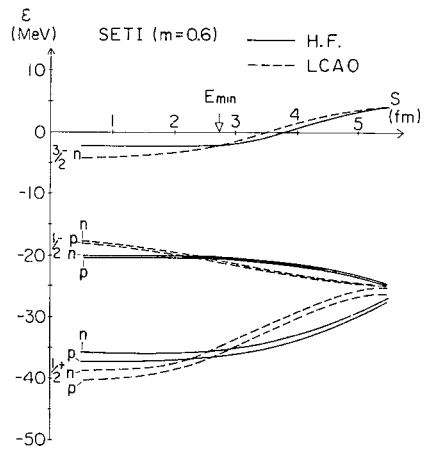

Fig. 2. Single-particle energies ε vs. cluster separation. $\phi_{3/2^-}$ orbital is occupied by the last neutron. $E_{\min}$ denotes the minimum point of the total energy.

tions in the H.F. calculations, which is in contrast to the normal parity states. This may imply that the truncated space is not so enough for the non-normal parity state as for the normal parity states, although the non-normal parity state has a distinct cluster structure. Thus it is well expected that the α-cluster structure is not destroyed by the presence of the valence neutron and that the simple LCAO approximation gives good descriptions to this nucleus.

In the following, we summarize properties of single-particle states obtained. Single-particle levels are shown in Fig. 2. The energy difference between the lowest two occupied levels with the same isospin is smaller than that in the simple shell model, which is given in the limit $S/b=0$. in the simple LCAO approximation. This is consistent with the results of the $(p, 2p)$ reaction.[17] The reason why neutron and proton levels split is that the single-particle Hamiltonian used in the present calculations depends on the isospin through the nuclear density, even if without the Coulomb interaction. Finally we analyze the single-particle orbitals by expanding them in terms of harmonic oscillator bases $\{|nlm\rangle\}$. In Table II the expansion coefficients are listed, together with those of the other models.[4),5)] It is found that the present results are very close to those of the P.H.F. calculation made by Bouten et al.[5)]

Table II. The probabilities of the occupied single-particle orbitals in harmonic oscillator wave functions $\{|nlm\rangle\}$. For the extended Nilsson model $(N+6)$, parameters $\eta=+5.3$, $\mu=0.0$ and $\kappa=0.08$ are taken. For P.H.F. the state of $L=1$ is taken from Ref. 5). For LCAO $S=3.34$ fm is taken.

	$0s0$	$0d0$	other	$0p0$	$0f0$	other	$0p1$	$0f1$	other
$SU(3)$	1.0	0.0	0.0	1.0	0.0	0.0	1.0	0.0	0.0
Nilsson	0.978	0.021	0.001	0.903	0.036	0.061	0.973	0.025	0.002
P.H.F.	0.865	0.135	0.0	0.942	0.058	0.0	0.957	0.043	0.0
LCAO	0.819	0.117	0.064	0.932	0.027	0.041	0.819	0.140	0.041

§ 4. Energy spectra

In this section energy levels of ^{9}Be are calculated in the framework of the simple LCAO approximation, which has been found to be quite good in the preceding section. In the final nuclear spectra shown in Figs. 4, 5 and 6, we take into account the effects of the dynamical motions of center-of-mass of α-clusters,

which are expected to be important in such a weakly bound system as ^{9}Be.

First, total energy curves for nuclear states are investigated. K-band mixing is taken into account at each cluster separation. The resultant solutions are called adiabatic ones. It follows that the model wave functions become the weak-coupling configurations of $\alpha+^5$He ($j^\pi(^5\text{He})=1/2^-$, $3/2^-$) in the limit of large S/b. In the limit of small S/b they go naturally to those of the $SU(3)$ model with K-mixing. Results are shown in Fig. 3. The curve for each nuclear state has a minimum up to $J^\pi=9/2^-$, whereas in the $SU(3)$ model the highest spins are $9/2^-$ for $(\lambda\mu)=(31)$ and $13/2^+$ for $(\lambda\mu)=(60)$. These minimum points are apparently different for each parity of the nuclear states; $S^-_{\min}\simeq 3.3$ fm and $S^+_{\min}\simeq 4.4$ fm. It is worth while noticing that the degree of clustering in the positive parity states is more distinct than in the ground band of ^{8}Be. The insufficiency of the absolute binding energy and the steepness of the energy curves in comparison with the case of ^{8}Be are mainly due to the odd-state repulsion of the effective force.

The relative motion between α-clusters is solved by the GCM. In solving Eq. (5), we use five and seven mesh points from the point 1.5 fm by the step 1.0 fm for the normal and non-normal parity states respectively. As for ^{8}Be, we use the same mesh points as those for the normal parity states. Resultant energy levels are compared with experiment in Fig. 4, together with those of ^{9}B. It is clear at a glance that they are in good agreement with experiment, not only in the normal parity states but also in the non-normal parity states. Furthermore, the present calculation reproduces the Coulomb energy difference observed between the ground states of ^{9}Be and ^{9}B.

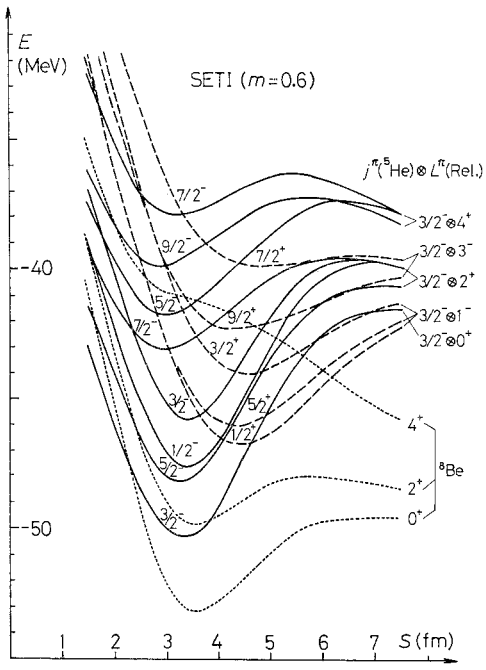

Fig. 3. Total energy curves for each angular momentum J^π. For ^{8}Be the value of the variational parameter b is 1.37 fm. Rel. stands for the relative motion between α and ^{5}He.

As shown in Fig. 4, the present calculation predicts: (a) a $9/2^-$ member of the $K^\pi=3/2^-$ ground band at about 10 MeV, but no experimental candidate observed yet, (b) a $7/2^-$ member of the $K^\pi=1/2^-$ band may correspond to the 11.28 MeV state, which is considered to be a mirror state of the $(7/2)^-$ level at 11.75 MeV in ^{9}B, (c) a $5/2^-$ member of the $K^\pi=1/2^-$ band may correspond to the 7.94 MeV state, (d) a $3/2^-$ member of the $K^\pi=1/2^-$

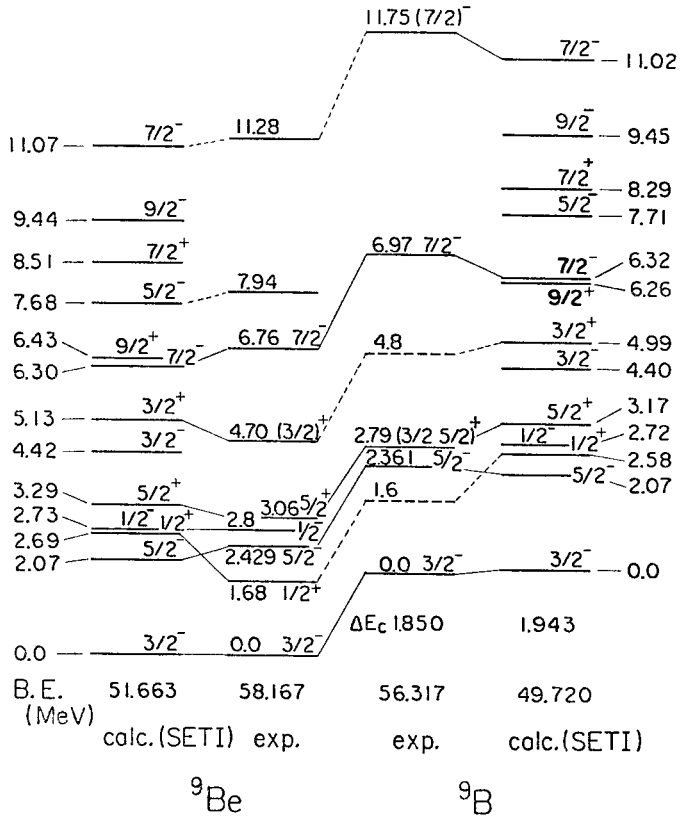

Fig. 4. The theoretical and experimental energy spectra of ^{9}Be and ^{9}B. B.E. stands for the binding energy and ΔE_c the energy difference between ^{9}Be and ^{9}B. The values of $\langle r^2\rangle^{1/2}$, Q and μ obtained for ^{9}Be are 2.62 (2.46 ± 0.11)fm, $5.76(6.5^{+0.9}_{-0.6})$fm^2 and -1.23 (-1.1776) n.m. respectively, where the values in parentheses are experimental ones.

band in the neighborhood of the $3/2^+$ level, so precise measurements of magnetic transitions to this energy region are strongly desired.

As for the non-normal parity states, the present results are also shown in Fig. 4. The results are very similar to those of the other models.[6),18)] The excitation energies of the states, however, are well reproduced in the present calculations, although the $1/2^+$ state is predicted to be somewhat higher than experiment, which is probably due to the restriction of the model space used. The present calculation does not predict stable second $1/2^+$, $3/2^+$ and $5/2^+$ states which are predicted by a weak-coupling model.[6)]

Overlaps between the GCM solutions and the adiabatic ones at minima are listed in Table III, together with the energy gains due to the G.C. calculations. As a whole the overlaps with the dominant simple LCAO bases are fairly large. There exist some other large ones, but they come mainly from the overlaps between the bases themselves. This means that the obtained levels can be classified into

Table III. Comparison of GCM solutions with the wave functions at the energy minima. $S_{\min}$, $E_{\min}$ and ΔE are an energy minimum point, a minimum energy and a difference, $\Delta E = E_{\min} - E_{GCM}$, respectively, where E_{GCM} is an eigenenergy of Eq. (5). The fifth column is overlapping between the GCM solution and the adiabatic one $|\min\rangle$. The latter three columns are overlappings between the GCM solution and the simple LCAO basis at a minimum point, where $|1/2(0)\rangle$ denotes a wave function $|K(\Lambda)\rangle$ at a minimum point.

J^π	$S_{\min}$(fm)	$E_{\min}$(MeV)	ΔE(MeV)	$\langle$GCM$\|\min\rangle$	$\langle$GCM$\|1/2(0)\rangle$	$\langle$GCM$\|1/2(1)\rangle$	$\langle$GCM$\|3/2(1)\rangle$
0^+(^{8}Be)	3.68	−53.27	2.44	−0.8736	—	—	—
$3/2_1^-$	3.34	−50.37	1.29	0.9661	−0.0344	−0.1997	−0.9621
$5/2_1^-$	3.29	−48.16	1.43	0.9593	−0.0413	−0.4677	−0.9357
$7/2_1^-$	2.95	−43.13	2.23	−0.9147	0.0814	0.3249	0.9083
$9/2^-$	2.90	−39.83	2.37	−0.8998	0.0522	0.7260	0.8705
$1/2^-$	3.45	−47.67	1.26	−0.9665	−0.0550	−0.9602	—
$3/2_2^-$	3.45	−45.84	1.40	0.9580	−0.0977	−0.9339	0.0912
$5/2_2^-$	2.99	−41.80	2.18	−0.9259	−0.0083	−0.7887	0.1963
$7/2_2^-$	3.22	−37.90	2.70	−0.8732	0.1486	0.7954	−0.1583
$1/2^+$	4.43	−46.74	2.23	0.9152	0.8928	0.2022	—
$3/2^+$	4.58	−44.04	2.49	0.8936	0.8609	−0.1197	0.3493
$5/2^+$	4.33	−46.03	2.34	0.9044	0.8542	0.4120	0.4350
$7/2^+$	4.99	−39.92	3.24	−0.8471	0.7444	−0.1544	0.5768
$9/2^+$	4.40	−42.27	2.96	0.8622	0.8018	0.5374	0.5759

rotational bands with good K quantum numbers. The reasons why axial symmetries hold so well are due to strong effects of the spin-orbit force and the Pauli principle which restricts the motion of the valence neutron. The overlaps with the adiabatic solutions at minima are almost the same as in the case of ^{8}Be in magnitude, which has some influence on particle decay widths, especially of the non-normal parity and higher excited states. Analyses of them will be given in the forthcoming paper.

The dependence of energy levels on the Majorana exchange mixture m is shown in Figs. 5 and 6. The level structure is not strongly affected by m, but the energy difference between the normal and non-normal parity states depends on m rather strongly.

As for the spin-orbit force, both one-body and two-body forces give similar results. Results with one-body force are given in Fig. 7. The dependence on the strength ξ is different in each model. In the shell model,[18] $3/2_2^-$, $5/2_2^-$ and $7/2_1^-$ levels are predicted very closely and in the P.H.F. calculation[5] the order of $5/2_2^-$ and $7/2_1^-$ levels is reverse to the present prediction. Thus the differences are important in distinguishing the models, which are clearly seen in Fig. 8. But unfortunately experimental data are not sufficient for a definite conclusion.

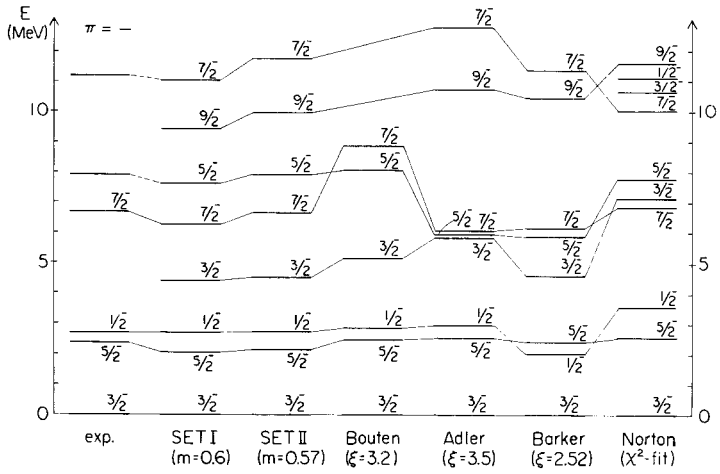

Fig. 5. Comparison of the present calculation with the other models in the normal parity states. For Bouten[5] the spin-orbit strength ξ is taken to fit to the $1/2^-$ level. Adler, Barker and Norton[18] are the shell model calculations.

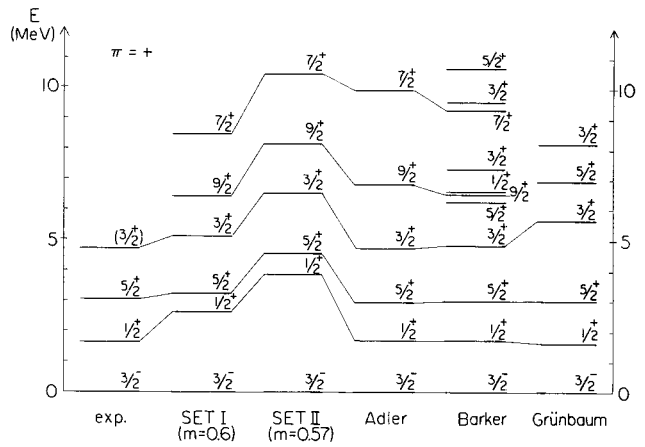

Fig. 6. Comparison of the present calculation with the other models in the non-normal parity states. Adler[15] is the shell model calculation. Barker and Grünbaum[6] are weak-coupling models.

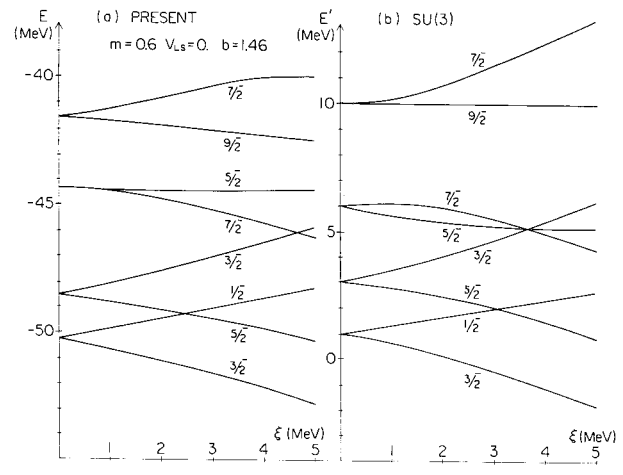

Fig. 7. The normal parity energy level scheme as a function of the spin-orbit strength ξ. (a) is the present result and (b) is the $SU(3)$ model, where the ordinate E' is the eigenvalue of the perturbation Hamiltonian $H' = 0.5L^2 - \xi\sum_i l_i s_i$.[18]

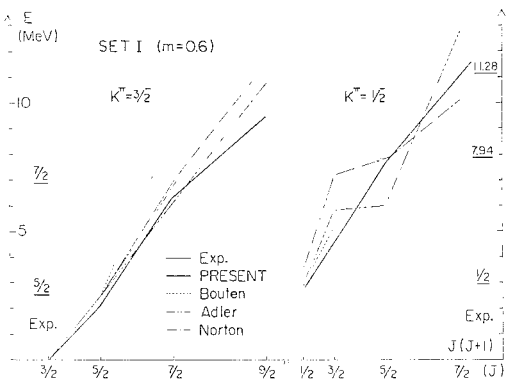

Fig. 8. The normal parity energy levels as functions of $J(J+1)$.

§ 5. Electromagnetic properties of the ground rotational band

As is well known, electromagnetic properties are useful in testing model wave functions. In this paper we restrict ourselves to analyses of the ground rotational band. Recently many interesting experiments[4),19)] have been carried out for the non-normal parity states. They will be dealt with in a forthcoming paper.

The r.m.s.-radius $\langle r^2\rangle^{1/2}$ of the ground state is determined by the elastic charge form factor. The value recently deduced by Bergstrom et al.[20)] is 2.46 ± 0.11 fm and the other data[3)] are within the above experimental errors. The quadrupole moment Q is determined by several experimental methods[3)] and values deduced are between 3.0 and 6.5 fm^2. From the atomic beam h.f.s., Blachman and Lurio[21)] have deduced $Q=5.26$ fm^2 with the Sternheimer correction. Contrary to the quadrupole moment, the magnetic moment μ has been measured with high accuracy, $\mu=1.1776$ n.m.[3)]

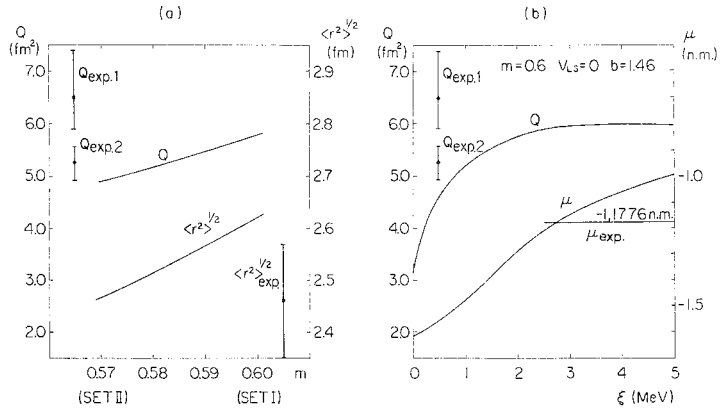

Fig. 9. (a) r.m.s.-radius $\langle r^2\rangle^{1/2}$ and electric quadrupole moment Q as a function of the Majorana exchange mixture m. $\langle r^2\rangle^{1/2}_{\rm exp.}$, $Q_{\rm exp.1}$ and $Q_{\rm exp.2}$ are taken from Refs. 20), 3) and 21) respectively. (b) Electric quadrupole moment Q and magnetic moment μ as a function of the spin-orbit strength ξ. $\mu_{\rm exp.}$ is taken from Ref. 3).

The dependence of $\langle r^2\rangle^{1/2}$ and Q on the Majorana exchange mixture m is shown in Fig. 9, where the depth V_{LS} is taken to reproduce the spin-orbit energy splitting. The values of $\langle r^2\rangle^{1/2}$ and Q are monotonically increasing functions of m and agree with experimental data in the range between 0.57 and 0.60. Bergstrom's value of $\langle r^2\rangle^{1/2}$ is reproduced with $m=0.57$. As for Q, the present model predicts 5.0 to 6.0 fm^2 with the above values of m, whereas the $SU(3)$ model gives 3.3 fm^2 at most within the consistency with $\langle r^2\rangle^{1/2}$.

The dependence of μ and Q on the strength ξ of one-body ls force is shown in Fig. 9, where m is fixed at 0.60. A calculated value of μ agrees with experimental data consistently with the spin-orbit splitting, if ξ is chosen between 2. and 4. MeV. In the same range of ξ, the calculated values of Q are almost stationary.

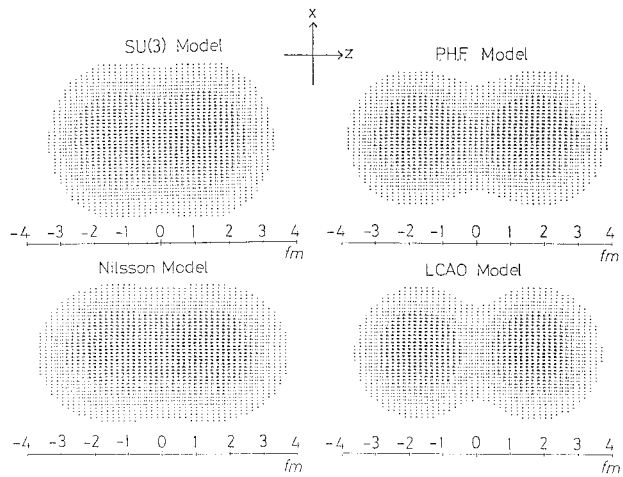

Fig. 10. The density distributions of the intrinsic states. The values of parameter b are 1.717 fm and 1.606 fm for the $SU(3)$ model and the Nilsson model, respectively. For the $SU(3)$ model $\langle r^2\rangle^{1/2}$ is fitted to 2.46 fm, and then Q is 3.3 fm^2. $S=3.34$ fm is taken in the present calculation.

Bernheim et al.[22] have measured the elastic charge form factor up to $q^2=9.$ fm^{-2}. As shown in Fig. 11, the present calculation achieves an overall fit to the experimental data as well as that of the $SU(3)$ model and the P.H.F. calculation by Bouten et al.,[5] whereas the extended Nilsson model by Slight et al.[4] has discrepancy at high momentum transfers. A failure of Kunz's classical α-particle model[7] is found to be due to an assumption of too large a deformation and due to a disregard of an overall antisymmetrization, as is clearly seen in Fig. 11. The differences among the models are intuitively understood by inspecting charge densities of the intrinsic states, for in strongly deformed nuclei, the concept of intrinsic state is good. Comparisons of the charge densities are made in Fig. 10. The present result is quite similar to Bouten's. Higher order deformations

should be added to the Nilsson potential.

As shown in Fig. 12, the present calculation reproduces experimental data on the inelastic form factor to the $5/2^-$ level at 2.43 MeV,[4),24),25)] and also the experimental transition probability $B(E2)$.[19),25)] Inelastic scattering to the $7/2^-$ level at 6.76 MeV has hardly been measured since Nguyen Ngoc et al.[25)] The calculated form factor is in good agreement with experiment. In the $SU(3)$ model the form factors and $B(E2)$'s cannot be explained at the same time, even if with effective charges. The present model predicts fairly strong inelastic scattering to the $9/2^-$ level, which is forbidden in the usual shell model. The calculated form factor is also shown in Fig. 12. Unfortunately experimental data are not available yet.

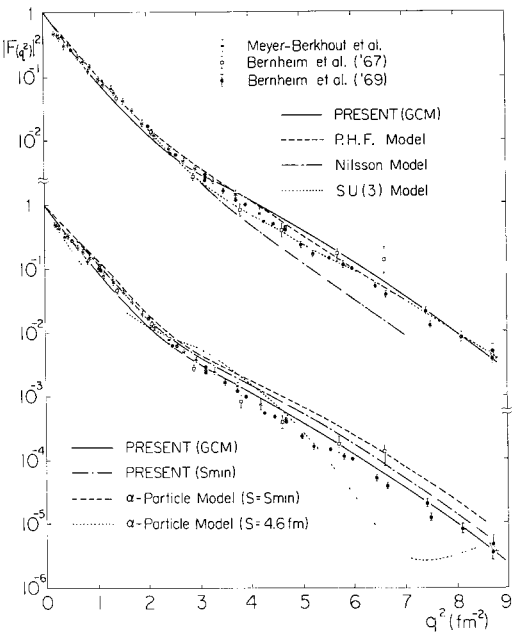

Fig. 11. In the upper part, elastic charge form factors are compared among several microscopic models, and in the lower the classical α-particle model[7)] is compared with the present calculations. The solutions with parameters SETI are used in the present calculations. PRESENT ($S_{\min}$) is the adiabatic solution at an energy minimum point. The value $S=4.6$ fm is determined by fitting the moment of inertia in the classical α-particle model.

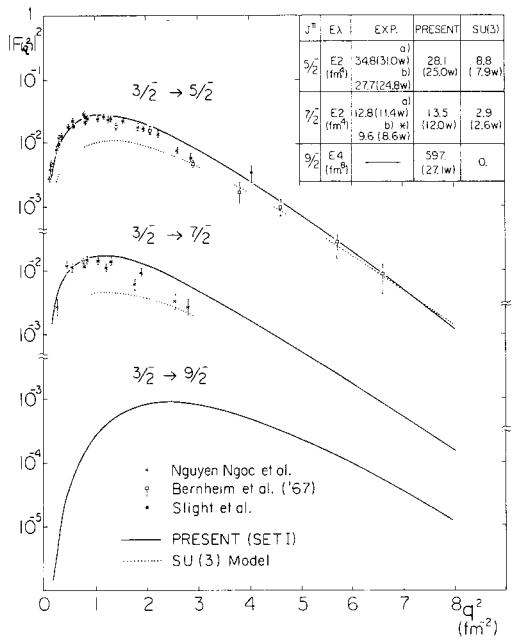

J^π	EX	EXP.	PRESENT	SU(3)
$5/2^-$	E2 (fm^4)	a) 34.8(31.0w) b) 27.7(24.8w)	28.1 (25.0w)	8.8 (7.9w)
$7/2^-$	E2 (fm^4)	a) 12.8(11.4w) b) w) 9.6 (8.6w)	13.5 (12.0w)	2.9 (2.6w)
$9/2^-$	E4 (fm^8)	——	597 (27.1w)	0.

Fig. 12. Inelastic charge form factors and electric transition probabilities. W denotes the Weisskopf unit. a) Ref. 25). b) Ref. 19).
*) Data deduced from $\Gamma_\gamma=0.082$ eV, $E_x=6.4$ MeV in Ref. 29).

§ 6. Conclusions

The molecular-orbital model has been extended to the odd-A system ^{9}Be. The motion of the valence neutron is described in terms of the LCAO and the relative motion of two α-clusters is dealt with by the GCM. The H.F. calculations have shown that both normal and non-normal parity states have stable α-cluster structures and that the latter has larger cluster separation than the former, which means the degree of clustering in ^{9}Be depends crucially on motions of the valence neutron.

Corresponding to motions of the valence neutron, several bands have been obtained with quite good K quantum numbers. The present investigation has predicted a stable $9/2^-$ member of the $K^\pi=3/2^-$ ground rotational band, which has not yet been observed experimentally. A $K^\pi=1/2^-$ band has been also predicted in a good rotational sequence, which is a different situation from the shell model prediction. Only the $1/2^-$ member has a corresponding level established experimentally at 2.78 MeV. $5/2^-$ and $7/2^-$ members have candidates in ^{9}Be or in ^{9}B, but a $3/2^-$ member has no evidence except strong magnetic transitions to 5 MeV region. The present calculation has predicted a reverse order of $5/2^-$ and $7/2^-$ levels to the prediction of the P.H.F. As for the non-normal parity states, experimentally observed $1/2^+$, $5/2^+$, $(3/2)^+$ levels have been reproduced at fairly good positions and will be improved by using a wider model space.

The present calculations have quite well reproduced the static properties of the ground state, that is, the r.m.s.-radius, the quadrupole and the magnetic moments. The enhanced electric transitions and the charge form factors for the members of the ground rotational band have been reproduced very well, whereas they cannot be explained by the $SU(3)$ model consistently.

It is concluded that the molecular model is quite successful in explaining not only the ground rotational band but also all the observed levels up to about 11. MeV of ^{9}Be systematically, on the basis of a simple and intuitive picture. Analyses of the other electromagnetic properties and particle decay widths will be given in a forthcoming paper.

Acknowledgements

This work was performed as a part of the annual research project on the "Alpha-like Four-Body Correlations and the Molecular Aspects in Nuclei" in 1975 and 1976 organized by the Research Institute for Fundamental Physics, Kyoto University, Kyoto.

The authors would like to express their thanks to Prof. J. Hiura and Dr. N. Takigawa for their discussion at the beginning of this study. They also thank the other members of the Nuclear Theory Laboratory of Hokkaido University for their encouragement.

Numerical calculations were made by FACOM 230-75 computer at Hokkaido

University and HITAC 8800/8700 computer at University of Tokyo.

Appendix

The basis wave functions in the present calculations are linear combinations of atomic orbitals, which are expressed, for example, as $|nlm, A\rangle$, a harmonic oscillator wave function around the point A. The axial symmetry is conserved, but the parity is not neccessarily conserved in the intrinsic states of ^{9}Be and therefore the bases are labelled as $\phi_{\Omega\pi}(nl, A\Sigma\tau_z)$ or $\phi_{\Omega\gamma}(nl, A\Sigma\tau_z)$ corresponding to the parity conserved case, $C_{\omega k}$ groups, or the parity non-conserved case, C_ω group, respectively, where Λ, Σ, Ω and γ are the projection along the symmetry axis of the orbital angular momentum, of the spin, of the total angular momentum and a suffix to distinguish the states with the same quantum numbers respectively.

In a parity conserved case, we obtain

$$\begin{aligned}
&\phi_{1/2^+}(0s, 0\ 1/2\ 1/2) = N_1(|0s0, A\rangle + |0s0, B\rangle)|\Sigma = 1/2\ \tau_z = 1/2\rangle,\\
&\phi_{1/2^+}(0p, 0\ 1/2\ 1/2) = N_2((|0p0, A\rangle - |0p0, B\rangle)|1/2\ 1/2\rangle\\
&\qquad\qquad - \lambda_{21}|\phi_{1/2^+}(0s, 0\ 1/2\ 1/2)\rangle)\\
&\phi_{1/2^-}(0s, 0\ 1/2\ 1/2) = N_4(|0s0, A\rangle - |0s0, B\rangle)|1/2\ 1/2\rangle,\\
&\phi_{1/2^-}(0p, 0\ 1/2\ 1/2) = N_5((|0p0, A\rangle + |0p0, B\rangle)|1/2\ 1/2\rangle\\
&\qquad\qquad - \lambda_{54}|\phi_{1/2^-}(0s, 0\ 1/2\ 1/2)\rangle),\\
&\phi_{3/2^-}(0p, 1\ 1/2\ -1/2) = N_8(|0p1, A\rangle + |0p1, B\rangle)|1/2\ -1/2\rangle, \quad \text{etc.}
\end{aligned} \tag{A·1}$$

In a parity non-conserved case, we obtain

$$\begin{aligned}
&\phi_{1/2_1}(0s, 0\ 1/2\ 1/2) = N^1|0s0, A\rangle|1/2\ 1/2\rangle,\\
&\phi_{1/2_2}(0s, 0\ 1/2\ 1/2) = N^2(|0s0, B\rangle|1/2\ 1/2\rangle - \lambda^{21}|\phi_{1/2_1}(0s, 0\ 1/2\ 1/2)\rangle),\\
&\phi_{3/2_1}(0p, 1\ 1/2\ -1/2) = N^7|0p1, A\rangle|1/2\ -1/2\rangle,\\
&\phi_{3/2_2}(0p, 1\ 1/2\ -1/2) = N^8(|0p0, B\rangle|1/2 - 1/2\rangle - \lambda^{87}|\phi_{3/2_1}(0p, 1\ 1/2\ -1/2)\rangle),\\
&\text{etc.}
\end{aligned} \tag{A·2}$$

The N_i's and N^i's are normalization constants and the λ_{ij}'s and λ^{ij}'s are the coefficients in the Gram-Schmidt orthonormalization procedure.

References

1) S. Okabe, Y. Abe and H. Tanaka, *Proceedings of International Conference on Nuclear Physics, Munich* (1973), Vol. 1, p. 116.
2) a) Prog. Theor. Phys. Suppl. No. 52 (1972); *Proceedings of the INS-IPCR Symposium on Cluster Structure of Nuclei and Transfer Reactions Induced by Heavy-Ions, Tokyo* (1975); *Proceedings of the Second International Conference on Clustering Phenomena in Nuclei,*

Maryland (1975).
b) J. Hiura, Y. Abe, S. Saito and O. Endo, Prog. Theor. Phys. **42** (1969), 277;
F. Nemoto and H. Bandō, Prog. Theor. Phys. **47** (1972), 1210; T. Sakuda, S. Nagata and F. Nemoto, Prog. Theor. Phys. **56** (1976), 1126.
3) F. Ajzenberg-Selove and T. Lauritsen, Nucl. Phys. **A227** (1974), 1.
4) A. G. Slight, T. E. Drake and G. R. Bishop, Nucl. Phys. **A208** (1973), 157.
5) M. Bouten, M.-C. Bouten, H. Depuydt and L. Schotsmans, Nucl. Phys. **A127** (1969), 177.
6) F. C. Barker, Nucl. Phys. **28** (1961), 96;
L. Grünbaum and M. Tomaselli, Nucl. Phys. **A160** (1971), 437.
7) P. D. Kunz, Ann. of Phys. **11** (1960), 275; Phys. Rev. **128** (1962), 1343.
8) J. Hiura and I. Shimodaya, Prog. Theor. Phys. **30** (1963), 585.
9) V. G. Neudatchin and Yu. F. Smirnov, Prog. in Nucl. Phys. **10** (1969), 275;
N. F. Golovanova and V. G. Neudatchin, Yadern. Fis. **13** (1971), 1248 (Soviet J. Nucl. Phys. **13** (1971), 718).
10) Y. Abe, J. Hiura and H. Tanaka, Prog. Theor. Phys. **49** (1973), 800.
11) D. M. Brink, *Proceedings of the International School of Physics "Enrico Fermi"* (1966) XXXVI, p. 247.
12) M. Bouten and P. van Leuven. Physica **34** (1967), 461.
13) D. L. Hill and J. A. Wheeler, Phys. Rev. **89** (1953), 1106;
J. J. Griffin and J. A. Wheeler, Phys. Rev. **108** (1957), 311.
14) A. B. Volkov, Nucl. Phys. **74** (1965), 33.
15) S. Nagata, private communication.
16) T. deForest, Jr. and J. D. Walecka, Adv. in Phys. **15** (1966), 1.
17) H. Tyrén, S. Kullander, O. Sundberg, R. Ramachandran and P. Isacsson, Nucl. Phys. **79** (1966), 321.
18) F. C. Barker, Nucl. Phys. **83** (1966), 418;
C. Adler, T. Corcoran and C. Mast, Nucl. Phys. **88** (1966), 145;
J. L. Norton and P. Goldhammer, Nucl. Phys. **A165** (1971), 33.
19) H.-G. Clerc, K. J. Wetzel and E. Spamer, Nucl. Phys. **A120** (1968), 441.
20) J. C. Bergstrom, I. P. Auer, M. Ahmad, F. J. Kline, J. H. Hough, H. S. Caplan and J. L. Groh, Phys. Rev. **C7** (1973), 2228.
21) A. G. Blachman and A. Lurio, Phys. Rev. **153** (1967), 164.
22) M. Bernheim, R. Riskalla, T. Stovall and D. Vinciguerra, Phys. Letters **30B** (1969), 412.
23) U. Meyer-Berkhout, K. W. Ford and A. E. S. Green, Ann. of Phys. **8** (1959), 119.
24) M. Bernheim, T. Stovall and D. Vinciguerra, Nucl. Phys. **A97** (1967), 488.
25) H. Nguyen Ngoc, M. Hors and J. P. Y Jorba, Nucl. Phys. **42** (1963), 62.